RADIO SCIENCE, VOL. 38, NO. 4, 1077, doi:10.1029/2002RS002686, 2003

Ionospheric *D* region electron density profiles derived from the measured interference pattern of VLF waveguide modes

Geoffrey Bainbridge

SRI International, Menlo Park, California, USA

Umran S. Inan

Space, Telecommunications, and Radioscience (STAR) Laboratory, Stanford University, Stanford, California, USA

Received 22 March 2002; revised 2 May 2003; accepted 4 June 2003; published 16 August 2003.

[1] The altitude profile of electron density in the *D* region is determined using an array of GPS-phase-referenced VLF receivers, allowing for the simultaneous broadband (i.e., phase coherent) measurement of a 24.0 kHz signal at multiple sites ranging in propagation path length from 3060 to 3353 km. Measured data are compared with results of model calculations for four electron density profiles used in previous work, assuming a single density profile to be in effect along the entire signal path from transmitter to receiver. Interpolation between model profiles is used to find a new profile which best fits the data. Phase coherent measurements over a range of path lengths also allow for the identification of the parameters for individual waveguide modes. Measured mode parameters agree with model calculations, within the limitations imposed by the configuration of the present array. A methodology of analysis and the required set of measurements is described, which would allow the decomposition of a VLF signal into all of its constituent waveguide modes, and accurate measurement of the characteristic parameters of each mode, namely phase velocity, attenuation rate, amplitude, and phase. *INDEX TERMS:* 0624 Electromagnetics: Guided waves; 2494 Ionosphere: Instruments and techniques; 2447 Ionosphere: Modeling and forecasting; 0689 Electromagnetics: Wave propagation (4275); *KEYWORDS:* array, ionosphere, waveguide

Citation: Bainbridge, G., and U. S. Inan, Ionospheric *D* region electron density profiles derived from the measured interference pattern of VLF waveguide modes, *Radio Sci.*, *38*(4), 1077, doi:10.1029/2002RS002686, 2003.

1. Introduction

[2] Measurements of the amplitude and phase of VLF signals propagating in the Earth-ionosphere waveguide have long been used effectively for remote sensing of the lower ionosphere. VLF sounding is a sensitive tool for the measurement of ionospheric conductivity (i.e., electron density and temperature), especially at altitudes below 90 km [e.g., *Sechrist*, 1974], and in recent years has been extensively utilized to study a variety of lower ionospheric disturbances, including those associated with lightning discharges [e.g., *Inan et al.*, 1992; *Burgess and Inan*, 1993], heating by HF [*Barr et al.*, 1985; *Bell et al.*, 1993] and VLF waves [*Rodriguez and Inan*, 1994], the auroral electrojet [*Kikuchi and Evans*, 1983; *Cummer et al.*, 1994, 1997], and relativistic electron precipitation enhancements [*Demirkol et al.*, 1999]. Computer-based models of VLF propagation and scattering are now available [*Pappert and Morfitt*, 1975; *Poulsen et al.*, 1990, 1993a, 1993b; *Smith and Cotton*, 1990; *Ferguson and Snyder*, 1990; *Baba et al.*, 1998; *Nunn et al.*, 1998] so that the VLF method can be quantitatively used to interpret ionospheric signatures of electron precipitation events [*Lev-Tov et al.*, 1996]. However, quantitative application of VLF remote sensing is complicated by the fact that the subionospheric VLF signal generally (except for specific cases such as long all-sea-based paths [e.g., *Inan et al.*, 1985]) consists of a multiplicity of waveguide modes, the relative amplitudes and phases of which are not known. Until recently, there was no easy way to measure the waveguide mode structure of VLF signals, due to the impracticality of conducting phase coherent measurements at distant sites.

[3] The VLF waveguide mode structure, and therefore the amplitude and phase of the total signal at particular receiver sites can in principle be predicted using theoretical models of VLF propagation [e.g., *Rodriguez and*

0048-6604/03/2002RS002686$11.00

Figure 1. The HAIL VLF receiver array with great-circle signal paths to U.S. Navy VLF transmitters (labeled by call sign and frequency).

Inan, 1994; *Cummer*, 2000], assuming that the electron density profile of the lower ionosphere is known along the propagation path. With the availability of GPS-based timing, and technological advances that facilitate simultaneous acquisition of wideband VLF data at multiply distributed sites, it is now possible to measure and compare phase (as well as amplitude) at distant sites, and invert the data to find an electron density profile. In this paper, we report the results of initial measurements of ionospheric electron density profiles realized with the Stanford University network of 13 VLF receivers situated along a north-south line in the central United States, known as the Holographic Array for Ionospheric Lightning (HAIL) (see Figure 1). HAIL receives signals from VLF communication transmitters operated by the U.S. Navy and records the wideband RF waveform in the 10–40 kHz band with a sampling frequency of 100 kHz. The time reference for the data comes from a GPS receiver at each site, providing an absolute time accuracy of ±40 ns, and a drift rate of less than 10^{-12}. The GPS unit outputs sample-synchronization pulses at a rate of 100 kHz, which trigger the A/D card, so that each data sample is phase-referenced to the GPS clock. This allows for a ±0.3° phase determination for a noise-free 24.0 kHz signal.

[4] One of the best defined signals received by HAIL originates at the NAA transmitter, broadcasting with a radiated power of ~1 MW at 24 kHz from Cutler, Maine. The HAIL receivers use magnetic loop antennas, with the loop axis pointing northwest, in order to maximize the reception of the signal arriving from NAA in the northeast. Other signals received by HAIL include: NPM (Lualuauei, Hawaii; 21.4 kHz), NLK (Jim Creek, WA; 24.8 kHz), NLD (25.2 kHz, North Dakota), and NAU (40.75 kHz, Puerto Rico). The bulk of the data acquired by HAIL consists of the detected amplitude and phase of the various transmitter signals, digitally extracted in real-time and recorded typically with 50 Hz (20 ms) resolution to be used for measurement of transient ionospheric disturbances which occur in association with lightning discharges. However, the fact that the receiver outputs are directly sampled at 100-kHz also provides the opportunity to record the signal in broadband form, retaining its full waveform with maximum resolution in amplitude and phase. Such data are typically only acquired in a highly selective manner (e.g., 1 s every hour), due to limitations in data storage. Nevertheless, the simultaneous broadband (phase coherent) measurement at multiple sites allows the HAIL array to be used as a VLF interferometer. Ultimately, it may be possible to conduct interferometric measurements of transient and localized disturbances of the lower ionosphere, such as those produced by lightning discharges. However, such analyses are complicated by the fact that even in an undisturbed ionosphere, the signal is not a uniform plane wave, but rather consists of a sum of waveguide modes. During the daytime, when the free-electron density in the *D* region is relatively high, the lowest (the so-called

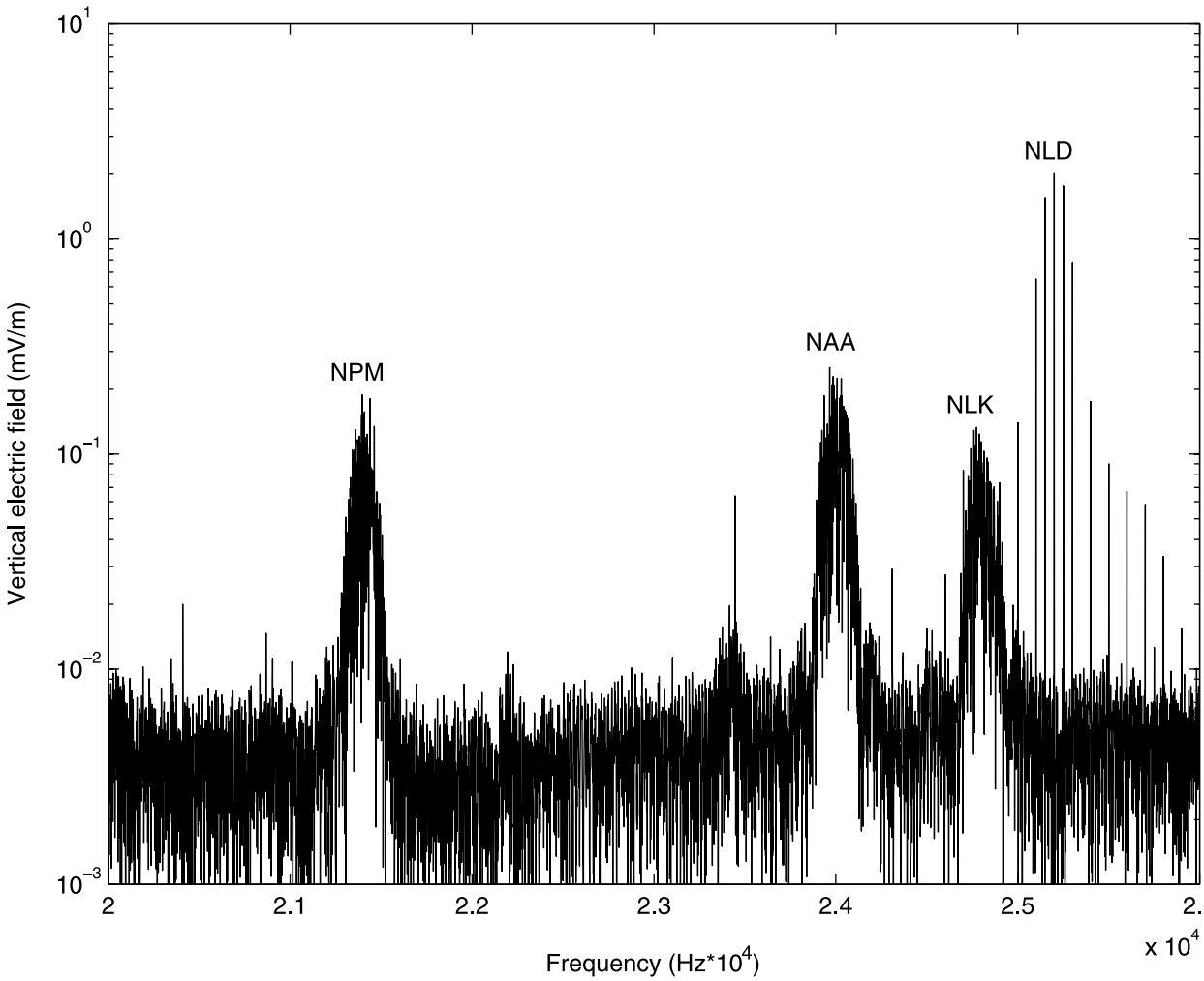

Figure 2. Amplitude spectrum of 1-s window of HAIL data, recorded at 22:15 UT (15:15 local time, i.e., midafternoon) on June 1, 2001, at Cheyenne, Wyoming. The frequency range is expanded to show the transmitters of interest.

quasi-transverse magnetic or QTM_1) mode dominates, and higher modes are strongly attenuated. At nighttime, on the other hand, the electron density is markedly lower, resulting in much lower attenuation, which allows the higher-order modes to propagate to long (many Mm) distances.

2. Data

[5] Figure 2 shows the amplitude spectrum of a 1-s window of typical daytime data. Signals from four transmitters may be seen. NPM, NAA, and NLK use the typical minimum shift-keying (MSK) modulation (typically at 200 bits per second), while the NLD transmitter, which was newly established and was undergoing testing at this time, is seen to be utilizing frequency shift keying (FSK) at this time. MSK modulation results in a continuous signal spectrum when averaged over time periods longer than the bit duration, whereas FSK appears as a set of discrete spectral ''lines.'' Figure 3 shows the corresponding phase spectrum. The phase appears random when averaged over a 1-s period, due to the modulation.

[6] On the other hand, when we subtract the phase spectrum observed at Cheyenne from that observed at a nearby site in Fort Collins, Colorado, we find that this phase difference is coherent across the band where the transmitter signals rise above the noise floor (see Figure 4). Note that since the NAA signal is more intense than the NLK signal (see Figure 2), it has a wider

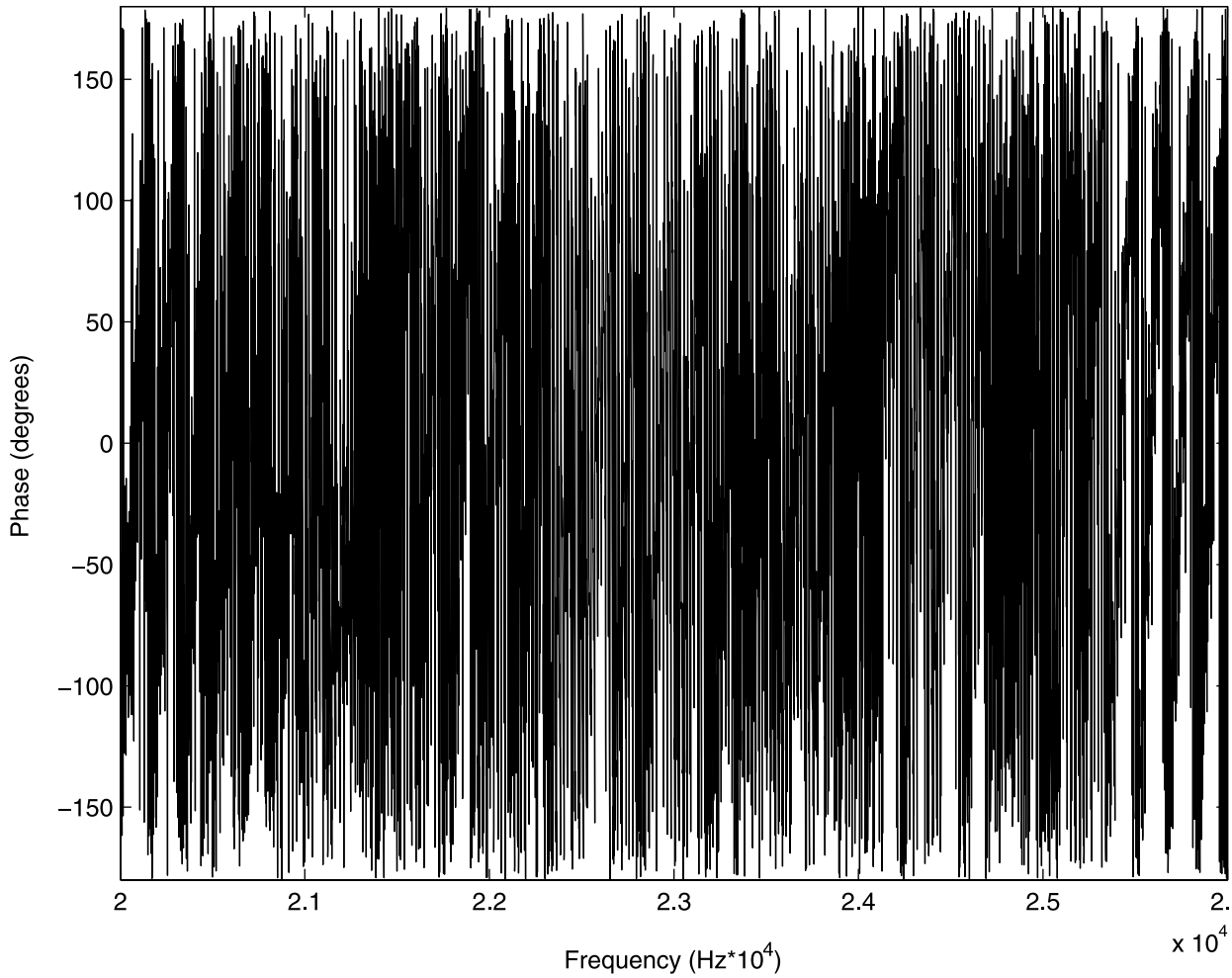

Figure 3. Signal phase versus frequency for the 1-s long data record shown in Figure 2.

bandwidth of coherent phase. Phase coherence is not visible for NLD, because its signal spectrum is not continuous in frequency (see Figure 2). Consequently, the NLD phase values are interspersed with and obscured by random phase values (due to noise) at other nearby frequencies.

[7] The phase coherence between distant sites as illustrated in Figure 4 indicates that the transmitter waveforms are basically similar at the two sites, except for a phase difference caused by propagation delay. The propagation path for VLF signals in the Earth-ionosphere waveguide is approximately the great-circle path over the surface of the Earth from the transmitter to each receiver. At each site, the total signal consists of a superposition of several individual waveguide modes. In those cases with one dominant mode, having much larger amplitude than the others, the phase difference is proportional to the great-circle distance from the transmitter to the receiver. Such is the case for the NAA-HAIL signal under daytime conditions, as is discussed later.

[8] We obtain amplitude and phase values for a particular transmitter signal by averaging spectral values within a 100 Hz window centered on the carrier frequency. Phase is always computed relative to Cheyenne, which is the northernmost station of the array, and also the closest to the NAA transmitter (i.e., shortest great-circle path). Referring to Figure 2, we define signal-to-noise ratio (SNR) as the ratio of the spectral power density at the center of the transmitter band to that of the adjacent noise floor. By this criterion, the mean SNR for NAA at the nine receiver stations is 27 dB. Amplitude and phase values computed from consecutive 1-s records are usually accurate (i.e., repeatable) within ±3% in amplitude and ±2 degrees in phase, although this range is sometimes exceeded, depending on local interference conditions at each site and atmospheric noise conditions

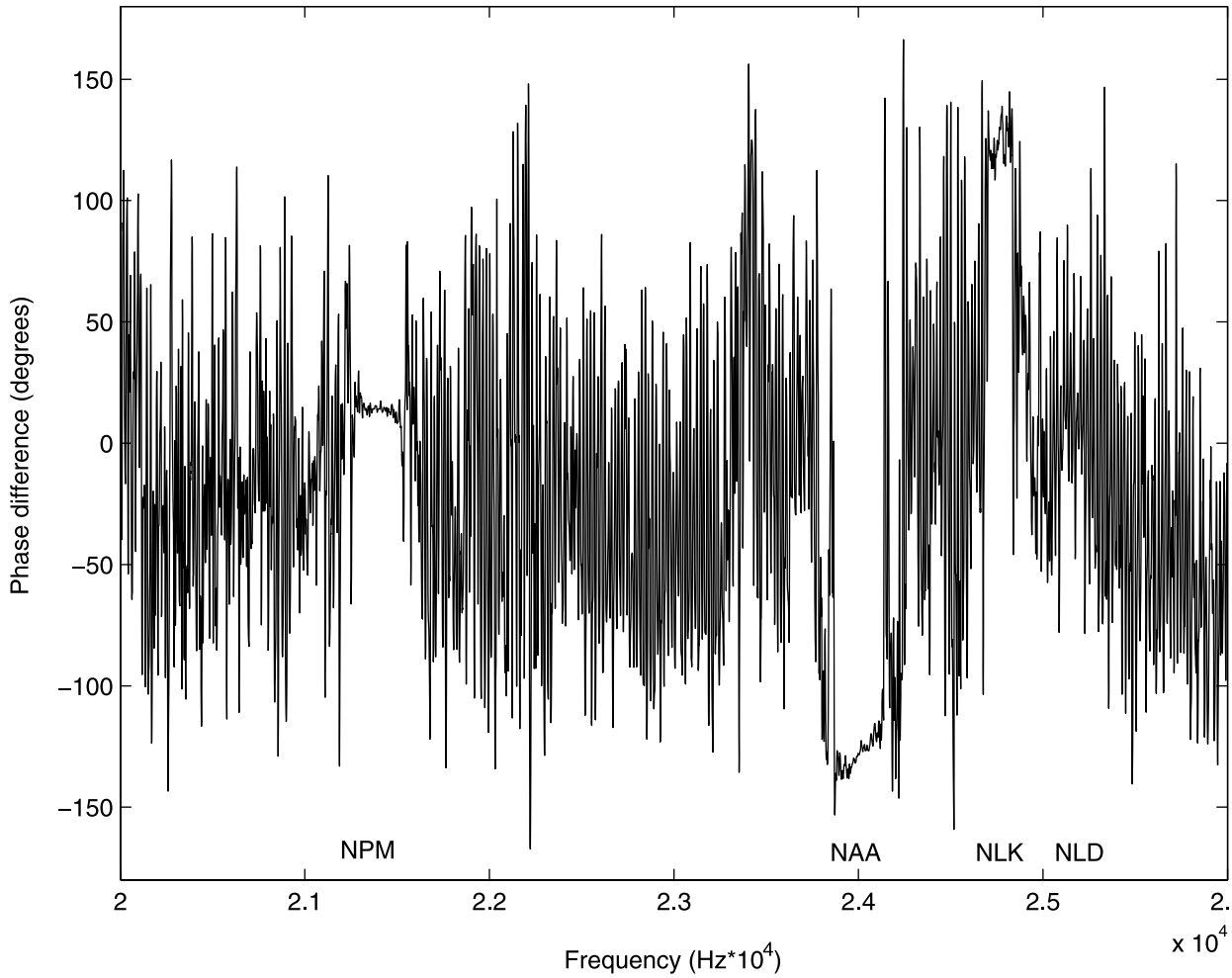

Figure 4. Difference in phase spectra for two simultaneous data records acquired at Cheyenne, WY, and Fort Collins, CO (22:15 UT, June 1, 2001).

(i.e., number and intensity of impulsive radio atmospherics due to nearby and distant lightning) on a particular day.

3. Waveguide Modes in Model Ionosphere

[9] Wave propagation in the Earth-ionosphere waveguide can be quantitatively modeled using the Long Wave Propagation Capability (LWPC) code developed by the Naval Oceans System Center [*Ferguson and Snyder*, 1990; *Ferguson*, 1998]. Based on the two-dimensional waveguide mode formulation of *Budden* [1962], which accounts for the curvature of the Earth, the *D* region electron density profile, and the Earth's magnetic field, the computer code was developed and experimentally verified by R. A. Pappert and his colleagues at the Naval Ocean Systems Center [*Pappert and Snyder*, 1972; *Pappert and Morfitt*, 1975; *Pappert and Ferguson*, 1986]. LWPC is presently used as the standard model of VLF propagation, both by the U.S. Navy, and by the ionospheric research community [e.g., *Cummer et al.*, 1997]. A three-dimensional version of the LWPC developed at Stanford University is used to quantitatively interpret subionospheric VLF signal perturbations associated with transient and localized ionospheric disturbances, such as those produced by lightning-induced electron precipitation [*Poulsen et al.*, 1990, 1993a, 1993b; *Lev-Tov et al.*, 1996], and by the heating of the lower ionosphere by VLF and HF transmitter signals [*Rodriguez and Inan*, 1994; *Bell et al.*, 1995].

[10] The ionosphere is described by an electron density profile as a function of height, which may also vary with latitude and longitude along the propagation path. LWPC uses the input ionospheric profile, together with a stored

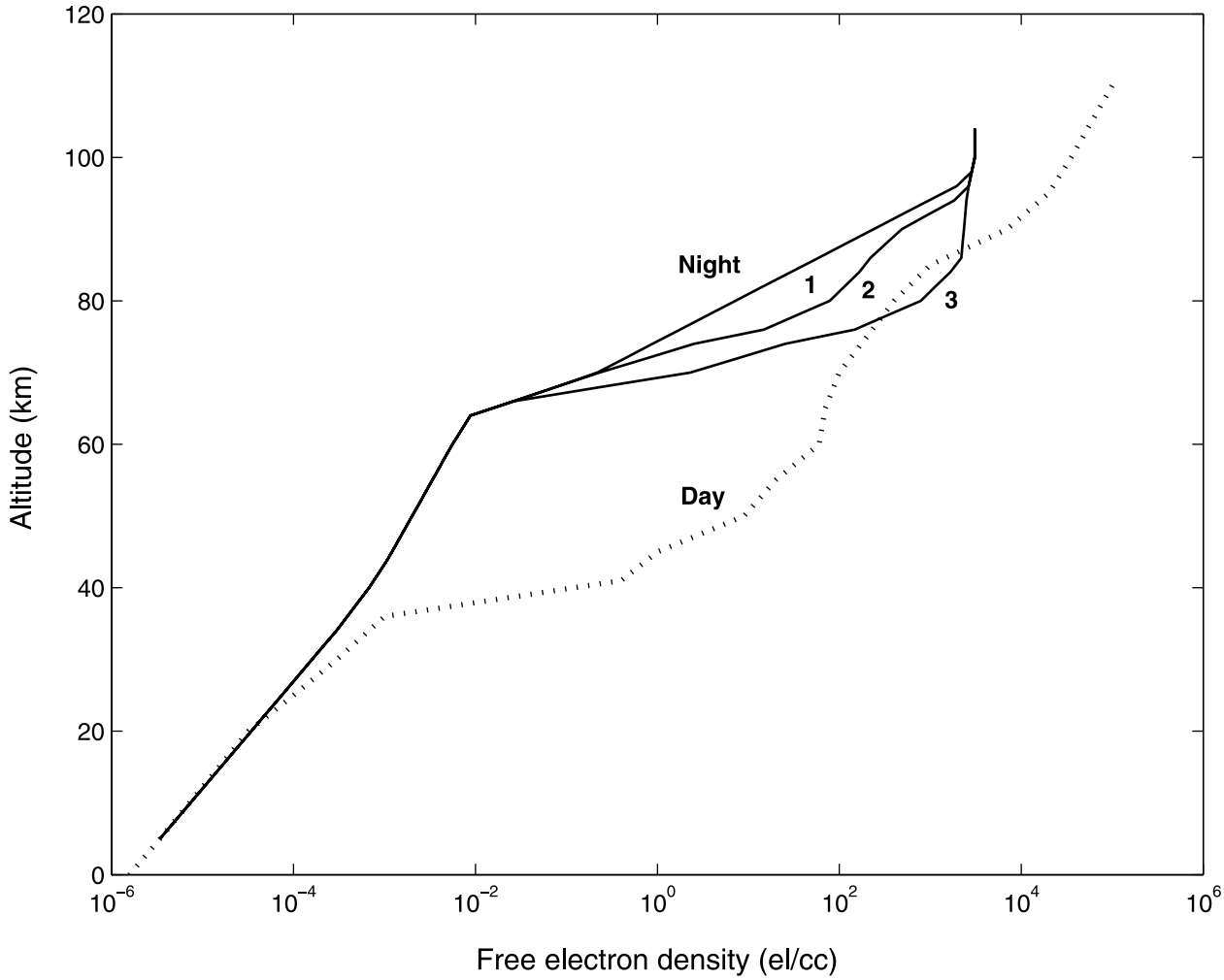

Figure 5. Ionospheric electron density profiles. Nighttime Profile 1 is a tenuous nighttime ionosphere represented by an exponential curve in the *D* region [*Wait and Spies*, 1964; *Wait*, 1966]. Profile 2 is a typical nighttime ionosphere [*Reagan et al.*, 1981], while Profile 3 is a dense nighttime ionosphere [*Inan et al.*, 1992].

map of the conductivity of the Earth's surface, to calculate the waveguide modes supported by the Earth-ionosphere waveguide over a given transmitter-receiver path. The code accounts for the initial excitation of these modes by the transmitter (based on an antenna model, ordinarily a small ($\ll\lambda$) vertical monopole antenna on the Earth's surface), and the resultant amplitude and phase of each waveguide mode all along the propagation path and thus at a given receiving site. In the standard version used in this study, LWPC uses a two-dimensional ionosphere model, assumes only forward scattering (equivalent to Born approximation), and assumes the scale of irregularities is much greater than a wavelength. The validity of these assumptions has been studied by *Baba et al.* [1998] and *Nunn et al.* [1998], who concluded that they are valid except in the vicinity of strong, localized scatterers (horizontal scale < 100 km and maximum electron density perturbation > 6 el/cc at 75 km altitude). The standard LWPC code is thus entirely adequate to model ambient ionospheric conditions on a continental scale.

[11] Figure 5 shows a typical daytime lower ionospheric profile [*Reagan et al.*, 1981], and three nighttime profiles. These four profiles have been used to represent lower ionospheric conditions in previous studies [e.g., *Lev-Tov et al.*, 1996].

[12] Tables 1 and 2 show the phase velocity (relative to the speed of light), attenuation constant, and relative

Table 1. LWPC Mode Parameters for Daytime Ionosphere Model

	Name	v_ϕ/c	α, dB/Mm	Relative E_z Amplitude
1	QTM_1	0.9977	−3.3	0.4557
2	QTE_1	0.9997	−7.0	0.0018
3	QTM_2	1.0061	−11.1	0.0585
4	QTE_2	1.0141	−22.1	0.0002
5	QTM_3	1.0249	−27.4	0.0028
6	QTE_3	1.0353	−62.6	0.0005
7	QTM_4	1.0518	−51.5	0.0026
8	QTE_4	1.0556	−79.3	0.0010
9	QTE_5	1.0894	−59.4	0.0024
10	QTM_5	1.0952	−98.4	0.0005

amplitudes of the vertical electric field for the first ten modes of the NAA signal received at the first station of the HAIL array (Cheyenne, WY), for typical daytime and nighttime profiles. Here we assume a laterally homogeneous ionosphere, i.e., the same electron density profile along the entire propagation path. Amplitudes have been normalized, such that the amplitude of the largest mode in the most typical nighttime ionosphere (Profile 2) is unity (see line 3, Table 2), while all other modes are scaled by the same factor. These calculated results indicate that the lowest-order mode (QTM_1) dominates during daytime, but that at nighttime there are 4 or 5 significant modes, with phase velocities ranging from 0.99-1.05 c and attenuation constants ranging from 0–10 dB/Mm. A similar mode constellation appears to be in effect for all three nighttime profiles.

[13] Figures 6 and 7 show the amplitude and phase of the total signal (i.e., the sum of all significant modes, as calculated using LWPC) as a function of distance from the transmitter, for all four ionospheric profiles. Note that the amplitude and the phase slope (i.e., $d\phi/dt$) of the daytime signal are nearly constant, and correspond, respectively, to the amplitude and phase velocity of the dominant QTM_1 mode (Table 1). The amplitude and phase slope of the nighttime signals are by no means constant, although they may appear constant over the limited extent (path length of 293 km) of the HAIL array. Clearly, the HAIL array is not positioned so as to capture the full details of the nighttime mode structure. Nevertheless, HAIL measurements provide enough information to distinguish between different lower ionospheric profiles, as shown in section 6.

4. Receiver Calibration

[14] The HAIL sites use vertical magnetic loop antennas, which measure one horizontal component of the magnetic field. We wish to compare this measured field component to the vertical electric field E_z computed by LWPC.

$$E_z = \eta H_y \sin\theta_i, \tag{1}$$

where H_y is the horizontal component of the magnetic field perpendicular to the direction of wave propagation, and θ_i is the angle of wave incidence with respect to the vertical. For the lower modes received by the HAIL array, $\sin\theta_i = c/v_\phi \cong 1$ (see Tables 1 and 2).

[15] The voltage recorded by the receiver A/D card is

$$V_r = G_r(f)\left[H_x \cos(\theta_r - \theta_t) + H_y \sin(\theta_r - \theta_t)\right], \tag{2}$$

where G_r is a complex, frequency-dependent receiver gain constant, H_x is the horizontal component of the magnetic field in the direction of propagation, H_y is the horizontal magnetic component in the perpendicular direction, θ_r is the direction of the receiver antenna loop axis, and θ_t is the direction of the transmitter with respect to the receiver. For the lower-order modes received by the HAIL array, the H_y component dominates. LWPC calculations indicate that for typical ambient ionospheres (as shown in Figure 5), $H_x/H_y \leq 2\%$. Therefore we use the approximate formula

$$V_r \cong G_r(f, \theta_t) \cdot H_y, \tag{3}$$

so as to easily relate our measurements to LWPC-calculated E_z values, via equation (1).

[16] All that remains is to find the calibration constant G_r for each receiver. Many factors affect the amplitude and phase response of equipment at a particular HAIL site, including amplifier gain and phase, antenna gain pattern and orientation, the local environment (nearby metal objects), cable losses, and the response of the A/D card. The HAIL array was set up over the course of a few years, and there were improvements in the receiver design over that time, as well as some modifications and repairs implemented in the field. There are two basic HAIL VLF receiver models: the older Tunable-VLF (or "TVLF") model (used at 5 sites), and the newer "Hail"

Table 2. LWPC Mode Parameters for Nighttime Profile 2

	Name	v_ϕ/c	α, dB/Mm	Relative E_z Amplitude
1	QTE_1	0.9956	−0.6	0.161
2	QTE_2	0.9962	−1.7	0.181
3	QTM_1	1.0017	−2.5	1.000
4	QTE_3	1.0054	−2.7	0.043
5	QTM_2	1.0141	−4.6	0.391
6	QTE_4	1.0203	−5.6	0.025
7	QTM_3	1.0342	−7.3	0.133
8	QTE_5	1.0422	−10.1	0.009
9	QTM_4	1.0627	−10.4	0.037
10	QTE_6	1.0725	−16.9	0.001

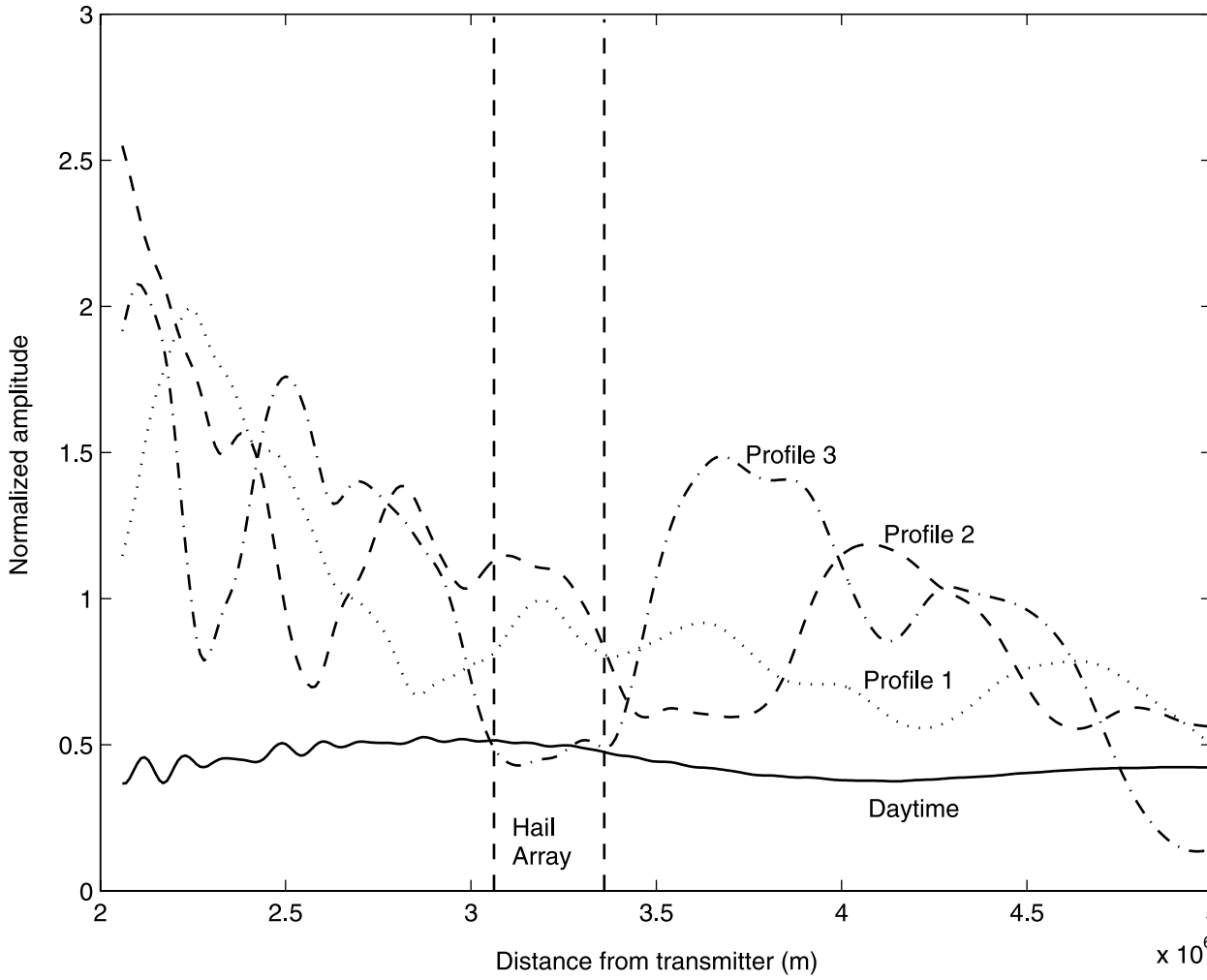

Figure 6. LWPC-calculated total amplitude (sum of modes) versus distance from the NAA transmitter for four different ionospheric profiles. Amplitudes have been normalized in the same way as in Tables 1 and 2, i.e., so that the amplitude of the largest mode in a typical nighttime ionosphere (Profile 2) is 1 at the nearest station of the HAIL array (Cheyenne, WY).

model (used at 8 sites). Within each model type, the receiver units are quite similar, except for one site (Las Vegas, NM), which uses a TVLF unit with a nonstandard antialiasing filter.

[17] Identical magnetic loop antennas are used at all sites. The antennas are oriented so as to maximize the NAA signal-to-noise ratio, meaning that the loop axis is roughly perpendicular to the direction of NAA, but since the local interference sources are different at each site, each antenna is oriented somewhat differently. This different alignment produces some variation in system gain. Furthermore, the antennas are located on the roofs of school buildings, and in this environment the magnetic field detected by the antenna may be perturbed by nearby pipes, wires, and sheets of metal.

[18] We need a calibration procedure that accounts for all of these factors, and incorporates them in a single lumped "calibration constant." We can do this using the single-mode signal received in the daytime as a reference to calibrate the multimode nighttime signal. For a single waveguide mode, the received voltage at a given receiver is

$$V_r = \frac{H_0 G_r(f, \theta_t)}{\sqrt{l}} \cdot 10^{(\alpha l/20)}, \qquad (4)$$

where H_0 is a source amplitude factor, l is the transmitter-receiver path length, α is the rate of attenuation in decibels per unit distance, and $G_r(f, \theta_t)$ is our calibration constant. The gain ratio of two receivers (for a given

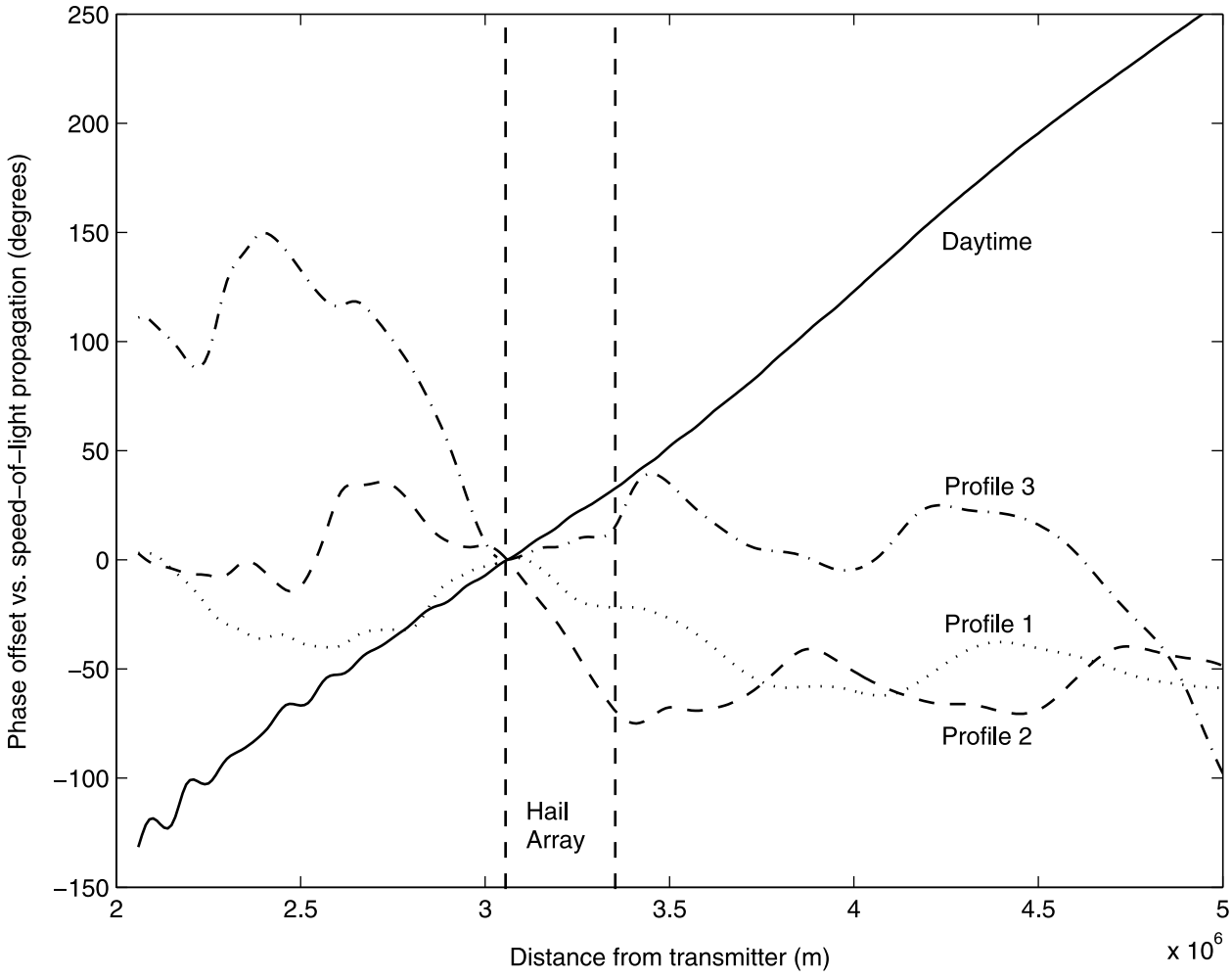

Figure 7. Phase of the LWPC-calculated total signal (sum of modes) versus distance from the NAA transmitter for four different lower ionospheric profiles. Phase has been normalized in two ways. The primary trend of phase versus distance is a straight line with slope close to c (speed of light in vacuum). In order to show small velocity variations, the speed-of-light trend (i.e., phase = $\omega \cdot$ distance/c) has been subtracted from the phase values. On this plot, positive slope indicates a phase velocity less than c. Also, the observation site with the shortest propagation path (Cheyenne) is taken as the zero-phase reference point, since in the course of HAIL measurements we do not know the absolute phase of the transmitter signal.

transmitter) can therefore be computed from the known path lengths, the measured signal amplitudes, and the LWPC-calculated attenuation rates, as follows:

$$\frac{G_2}{G_1} = \frac{\sqrt{l_2/l_1}}{10^{(\alpha(l_2-l_1)/20)}} \cdot \frac{V_2}{V_1}. \quad (5)$$

Note that (5) applies only to the case of a single waveguide mode. This is approximately the case for the daytime NAA signal received at HAIL, as shown in Table 1. Table 3 shows the relative amplitude of the NAA signal at various sites with respect to Cheyenne, recorded

Table 3. NAA Daytime Amplitudes and Station Gains, Relative to Cheyenne

Station	Amplitude	Gain	Type
Cheyenne, WY	1.00	1.00	Hail
Boulder, CO	1.20	1.25	Hail
Green Mountain, CO	1.01	1.06	Hail
Colorado Springs, CO	0.87	0.92	Hail
Walsenburg, CO	1.01	1.10	Hail
Fort Collins, CO	3.29	3.38	TVLF
Pueblo, CO	2.27	2.41	TVLF
Trinidad, CO	2.85	3.11	TVLF
Las Vegas, NM	1.64	1.92	modified TVLF

Table 4. Phase Offsets of Receivers, Assuming $v_\phi = 0.9977\ c$

Station	$\Delta\phi$	$k \cdot \Delta l$ (mod 360)	$\Delta\phi_0$	Receiver Type
Cheyenne, WY	0	0	0	Hail
Boulder, CO	189.4	192.5	−3.1	Hail
Green Mountain., CO	282.0	273.9	8.1	Hail
Colorado Springs, CO	12.1	8.0	4.1	Hail
Walsenburg, CO	244.4	242.2	2.2	Hail
Fort Collins, CO	286.1	147.4	138.7	TVLF
Pueblo, CO	242.2	120.4	121.8	TVLF
Trinidad, CO	252.2	140.6	111.6	TVLF
Las Vegas, NM	194.6	169.4	25.2	modified TVLF

at 22:15 UT (3:15 pm local time), on June 1, 2001. Assuming that the attenuation constant of the dominant daytime NAA mode is $\alpha = -3.3$ dB/Mm (as given by the LWPC model calculation), we can adjust these values to determine the relative gain factors of the receivers, also shown in Table 3. Note that the gain is similar for receivers of the same type, confirming the validity of our assumptions about the daytime signal.

[19] A similar procedure is used for phase calibration, once again based on the assumption of a single-mode signal in the daytime. For such a signal, the phase ϕ at a given site is a simple function of the transmitter-receiver path length l:

$$\phi = \phi_s + kl + \phi_0, \tag{6}$$

where k is the horizontal wave number of the dominant waveguide mode, ϕ_s is the phase of the source, and ϕ_0 is the phase offset of the receiver unit. The phase difference between two receiver stations is then given by

$$\Delta\phi = k \cdot \Delta l + \Delta\phi_0, \tag{7}$$

where we note that $\Delta\phi_0$ should be close to zero for two receivers of the same type.

[20] Table 4 shows that $\Delta\phi_0$ is indeed close to zero for receivers of the same type. It shows $\Delta\phi_0$ for nine receiver stations, taking the first station (Cheyenne, WY) as a phase reference, and using $v_\phi = 0.9977\ c$ (the phase velocity of the dominant NAA mode as given by the LWPC daytime model). After removing the path length effect (i.e., $k \cdot \Delta l$), the phase offsets of the Hail-type receivers with respect to Cheyenne are close to zero, and the phase offsets of the TVLF receivers form a separate cluster around 120° (except for Las Vegas, which has a modified TVLF system).

[21] This result shows that the value of v_ϕ as given by LWPC is approximately correct. Nevertheless, it may be possible to find an improved estimate. Instead of using $v_\phi = 0.9977\ c$, we can vary v_ϕ so as to minimize the variance of each cluster of Δv_ϕ values, i.e., make the HAIL group converge as closely as possible on zero, and the TVLF group converge on some other constant value. Implementation of such a procedure results in an optimum value of $v_\phi = 0.9975\ c$, very close to the value given by the LWPC model. The resultant minimum-variance Δv_ϕ values are very similar to those in Table 4.

[22] It must be noted that waveguide modes above the dominant QTM_1 are incorporated in the Δv_ϕ values. Table 1 indicates that the amplitude ratio of the second-largest QTM_2 mode to the dominant QTM_1 is 0.128. Other modes are small enough to be neglected. The phase of QTM_2 with respect to QTM_1 will have a uniform random distribution for an arbitrary set of receiver locations. Therefore the mean absolute phase deviation of the total signal due to the presence of QTM_2 will be $2/\pi * 0.128$ radians = 4.7 degrees. This corresponds well to the $\Delta\phi_0$ values observed for the Hail-type receivers. It seems likely that these phase deviations are due more to the QTM_2 mode than to the receiver response. Consequently, we take the phase offset of the Hail-type receivers to be zero and do not apply phase calibration, but for the TVLF receivers, which have much larger phase offsets, we use the $\Delta\phi_0$ values for calibration.

[23] Error in the final calibrated measurements is therefore due to the sum of noise and calibration errors, which are uncorrelated. We estimate that the noise error is ±3% in amplitude and ±2 degrees in phase, and that the calibration error is similar or larger, so that the total error is estimated to be at least ±5% in amplitude and ±3 degrees in phase.

5. Measured Amplitude and Phase Profiles

[24] Figures 8 and 9show five sets of calibrated amplitude and phase values measured on the HAIL array at half-hour intervals from 07:15 to 09:15 UT (nighttime, shortly before dawn) on June 4, 2001. The values for the first three times (07:15, 07:45, and 08:15 UT) are clustered together, but then a break occurs at 08:45 UT, when the Sun rises over the transmitter. This break is particularly apparent in the phase values. At 08:15 UT, the Sun shadow height over the NAA transmitter is 70 km, which is above the lower boundary of the daytime D layer, where most of the VLF energy is reflected (see Figure 5). At 08:45 UT, the Sun shadow has dropped to 17 km, and at 09:15 UT the transmitter itself is in daylight, although the receiver is still in shadow.

6. Fitting Nighttime Data to Ionospheric Profiles

[25] Figures 10 and 11 show the amplitude and phase values measured at 08:15 UT, compared with

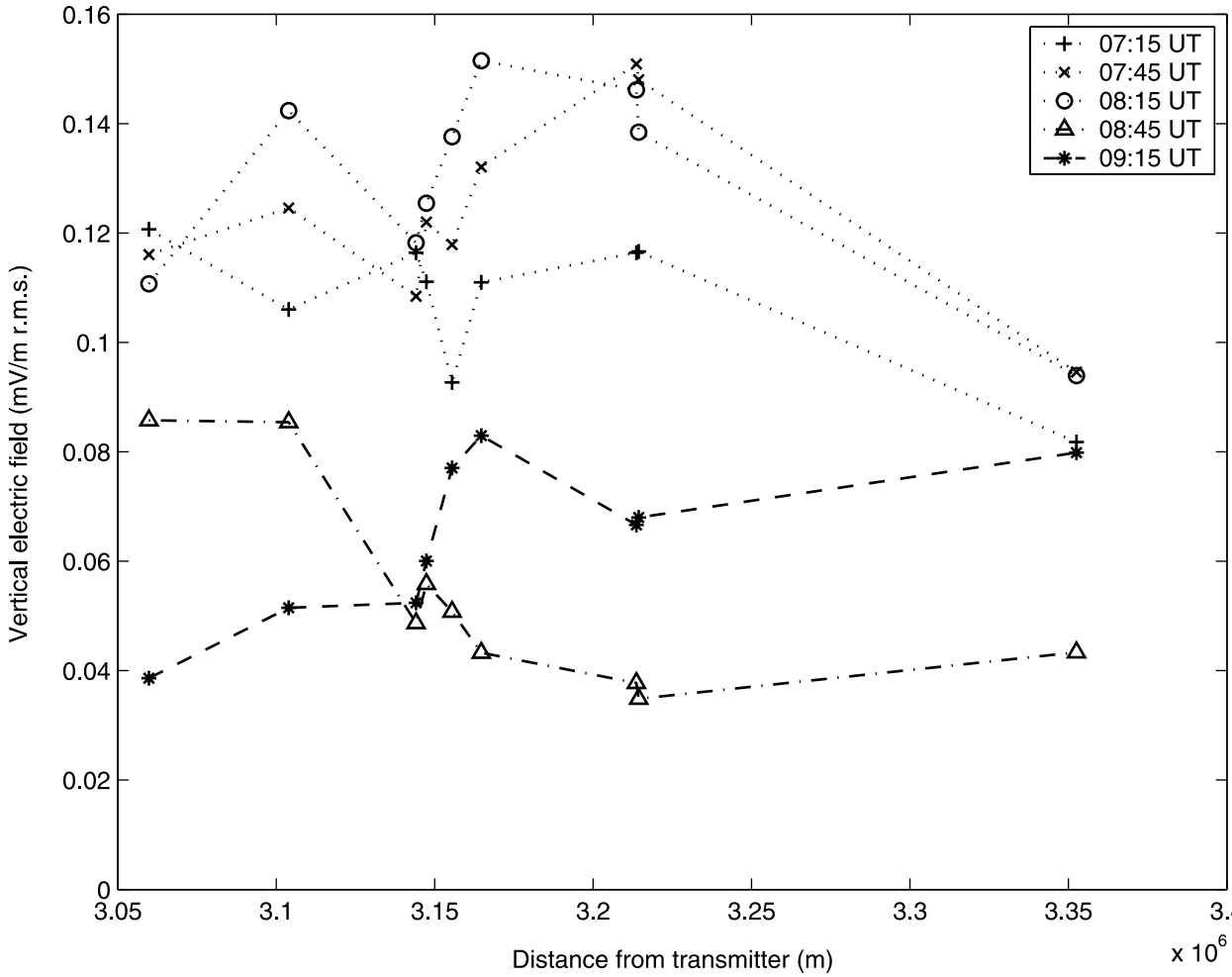

Figure 8. Signal amplitude versus distance from NAA transmitter, as measured by the HAIL array, at five half-hour intervals near dawn on July 4, 2001. For the first three measurements, the entire signal path is in shadow at *D* region altitudes; for the last two, the Sun has risen over the transmitter.

values calculated using the LWPC model, with different lower ionospheric density profiles. The time of 08:15 UT is the last measurement time before sunrise at the *D* layer altitudes, and was chosen for analysis because the average signal amplitude is highest at this time, so that the signal-to-noise ratio is maximized. Since the entire signal path is in shadow, we can still use a laterally homogeneous nighttime lower ionosphere model.

[26] The measured data points lie generally between the LWPC calculated values for Profiles 1 and 2, suggesting that a density profile that lies between these two profiles might provide a better fit. Trying different combinations of both linear and logarithmic interpolation, the following interpolated profile (see Figure 12) was found to give the best fit, in the sense of minimizing (in a mean-squared-error sense) phase differences with respect to the measured data:

$$N_e(h) = \exp(0.15\log(e_1(h)) + 0.85\log(e_2(h))), \quad (8)$$

where $N_e(h)$ is the electron density as a function of altitude. The best fit profile is only slightly different from Profile 2, which represents the nighttime electron density under typical conditions, based on past work. Nevertheless, it is evident that VLF phase and amplitude response is sensitive to such a slight change (i.e., a

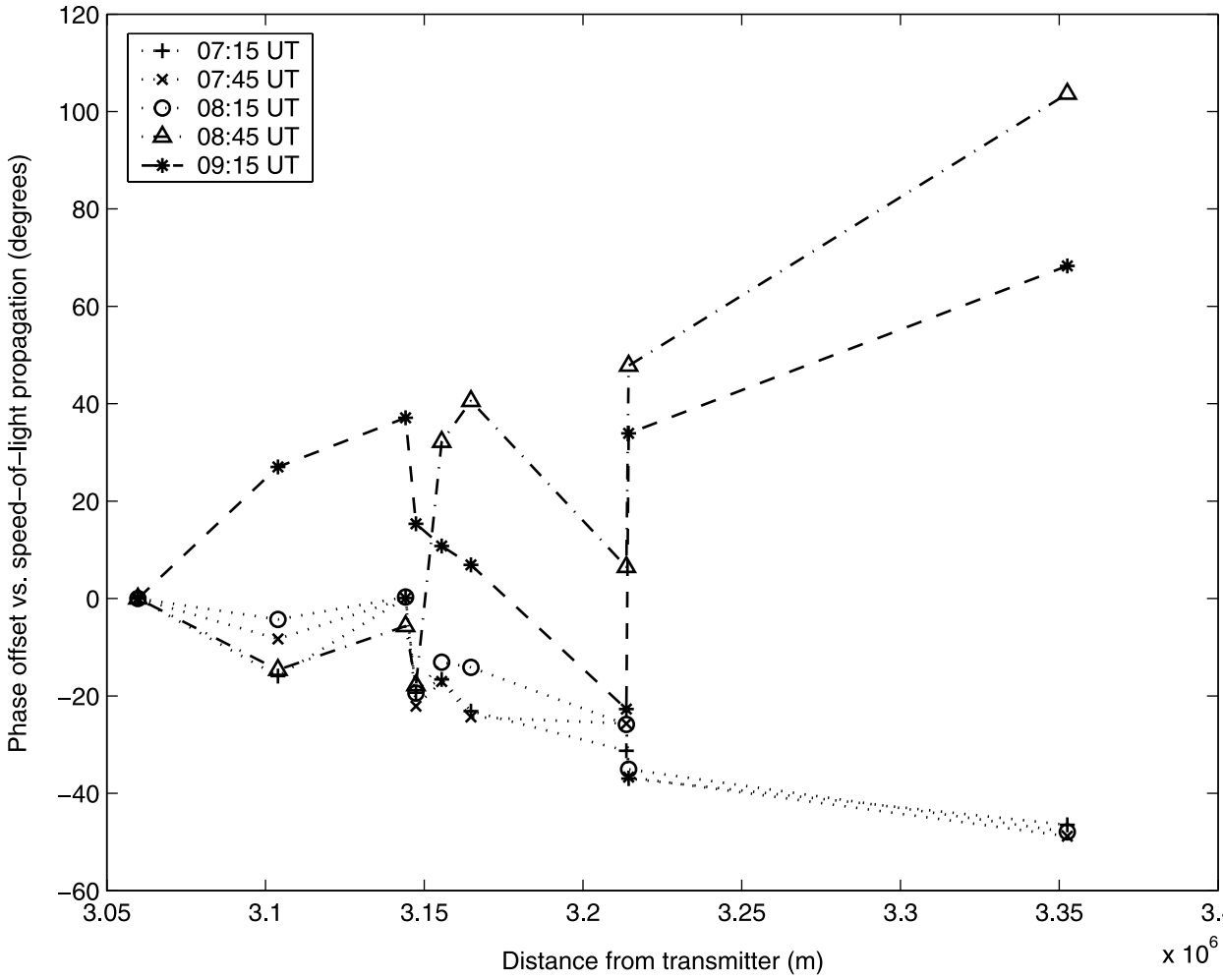

Figure 9. Signal phase versus distance from NAA transmitter, for the same data shown in Figure 8. Phase has been normalized in the same way as in Figure 7.

maximum of 30% change in electron density, or 55 versus 79 el/cc, at 80 km altitude).

[27] The mean absolute amplitude difference between the measured data and the amplitude values obtained using LWPC with the best fit profile is 10.6% (0.9 dB), while the mean absolute phase difference is 4.7 degrees. These values are nearly twice our previous estimates of minimum measurement error (±5% amplitude, ±3 degrees phase). Furthermore, we note from Figures 10 and 11 that the LWPC calculations call for a much smoother variation in amplitude and phase with distance than is shown in the data. The discrepancies between measured and calculated values may be due to measurement error (which may be larger than estimated) and/or lateral variations in the ionosphere.

[28] Table 5 shows the phase difference between the best fit profile for 08:15 UT and measured data from various times, before and after sunrise. A change in phase is detectable over the hour before sunrise; however, the change is less than the error in fitting the profile to the 08:15 UT data. Other data (not shown) indicate that the measured amplitude and phase values evolve slowly through the night, to the point where a significantly different ionospheric profile can be fitted. However, in this article we confine ourselves to demonstrating methods of measurement of ionospheric parameters, and leave the issue of ionospheric variability for future study. We simply note that geomagnetic conditions were quiet (Kp = 1+) over the period shown, and that the nighttime ionosphere was thus correspondingly stable.

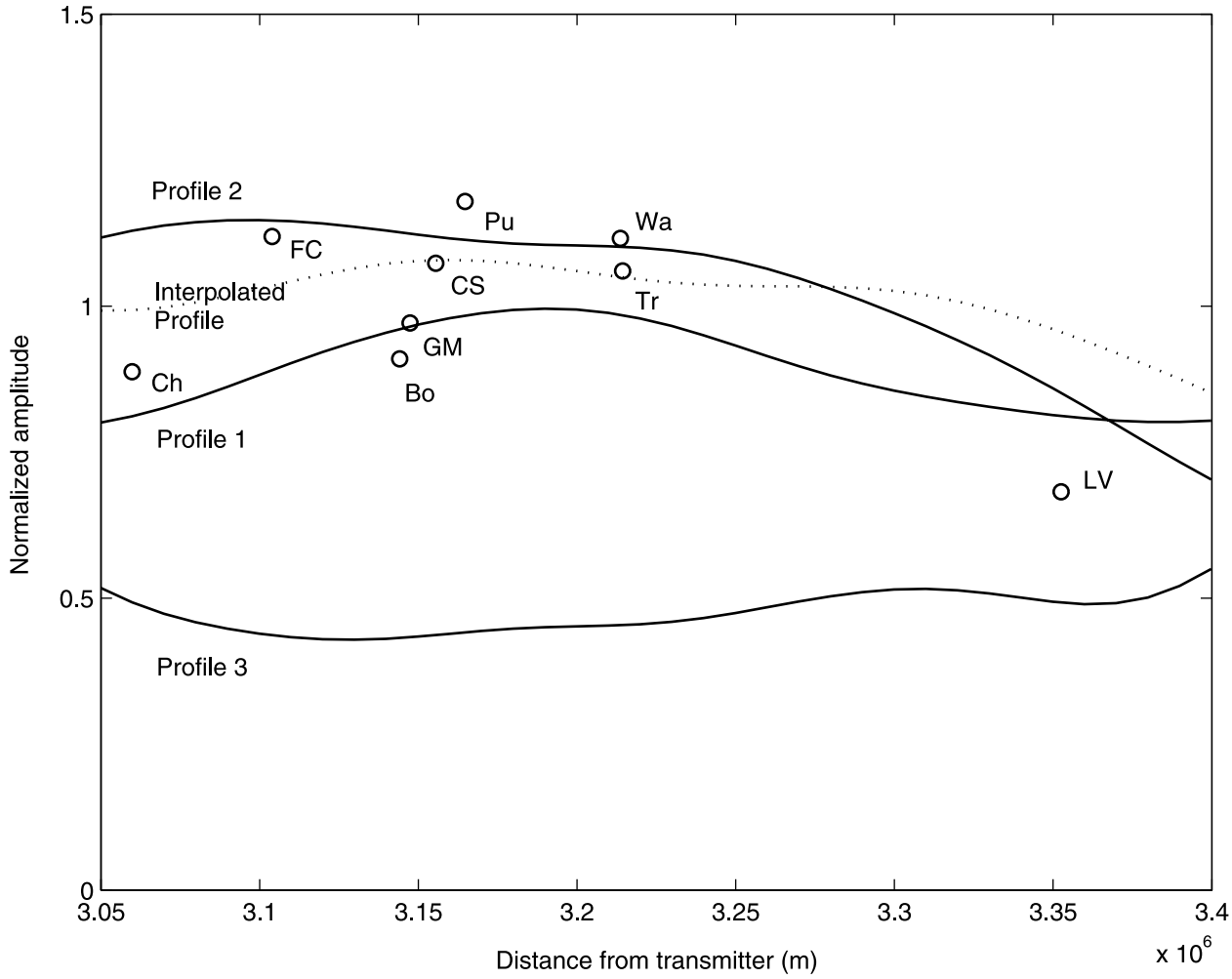

Figure 10. Normalized amplitude versus distance from NAA transmitter, showing both measured values (circles) and those calculated using the LWPC model. Each measured data point is identified by two letters, indicating the site name. Amplitudes have been normalized in the same way as in Figure 6. Profiles 1, 2, and 3 are the theoretical nighttime profiles shown in Figure 5. The interpolated profile which gives the best fit to the measurements is shown in Figure 12.

[29] By contrast the change at sunrise is dramatic. The state of the ionosphere has obviously changed, and we cannot simply solve for a new best fit profile, because the Sun has risen over the transmitter, while it is still nighttime over the receivers, and therefore the single-profile model no longer applies. *Pappert and Morfitt* [1975] used an earlier version of the LWPC code to implement a multiprofile model of the day-night terminator in the *D* region, and compared calculated with measured amplitude profiles. They obtained good qualitative agreement, in that the calculated and measured profiles had the same set of major peaks and nulls, colocated within 100 km on a 5000 km baseline. However, the amplitudes differed by up to 10 dB at some points in the profile. (Phase was not measured.) The complexity of the situation made it impractical to find a model which closely fit the data at all points. The same limitation still applies today. LWPC is a forward model, i.e., it calculates the VLF signal from a given ionosphere. The only way to find an inverse solution is by trial and error, and each iteration takes time to run. If the transmitter-receiver path is divided into segments, each with a different ionospheric profile, the total number of possible states grows exponentially.

[30] To overcome this limitation, we seek an inverse method to solve for ionospheric parameters directly from measured data. From multireceiver amplitude and phase measurements it is possible to find the VLF mode

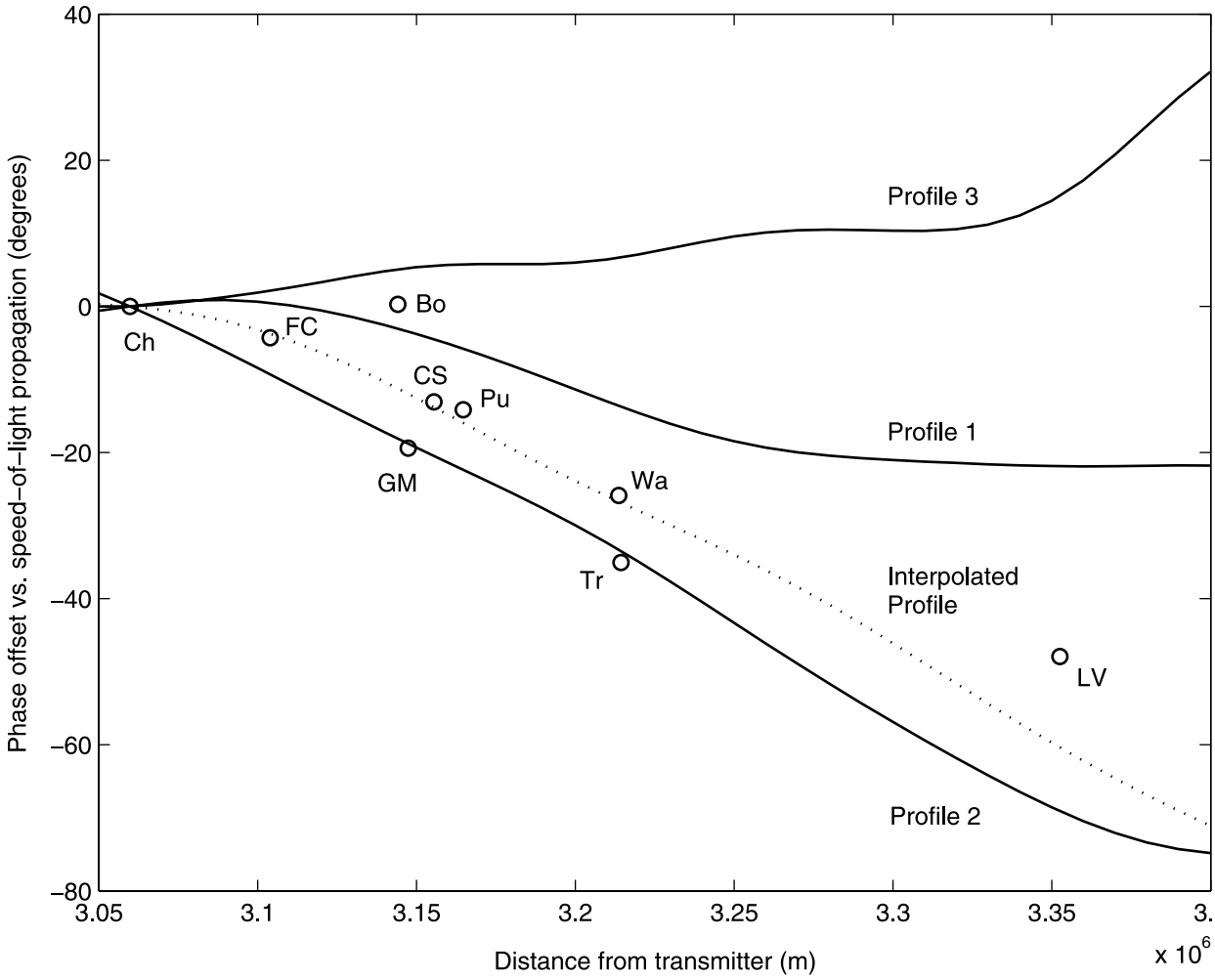

Figure 11. Normalized phase versus distance from NAA transmitter, for the same data as shown in Figure 10. Phase has been normalized in the same way as in Figure 7.

structure in the Earth-ionosphere waveguide, as described in the next section. This determination is not dependent on the assumption of a homogeneous ionosphere between source and receiver, or any particular assumption about the waveguide, except for the requirement of a homogeneous ionosphere over the length of the receiver array. Knowledge of the mode structure is a significant first step towards finding the state of an arbitrary ionosphere.

7. Measurement of VLF Waveguide Mode Structure

[31] Figures 6 and 7 indicate that the HAIL array captures some information about the constellation of modes propagating in the Earth-ionosphere waveguide. However, it is clear that the extent of the HAIL array samples only a segment of a larger interference pattern, which exhibits a nearly linear variation of amplitude and phase. Such a variation could have been just as easily viewed with data from just two or three sites. Sampling the full spatial frequency content of the amplitude pattern would require receivers spaced farther apart, and extended over a longer baseline.

[32] It is evident from Figures 6 and 7 that the mode interference pattern repeats (albeit with steadily reducing amplitude) every 1000 km or so, as the most significant modes move in and out of phase with respect to one another. Table 2 indicates that the most significant modes in the nighttime ionosphere are QTM_1 and QTM_2. For Profile 2, these modes are calculated to have phase

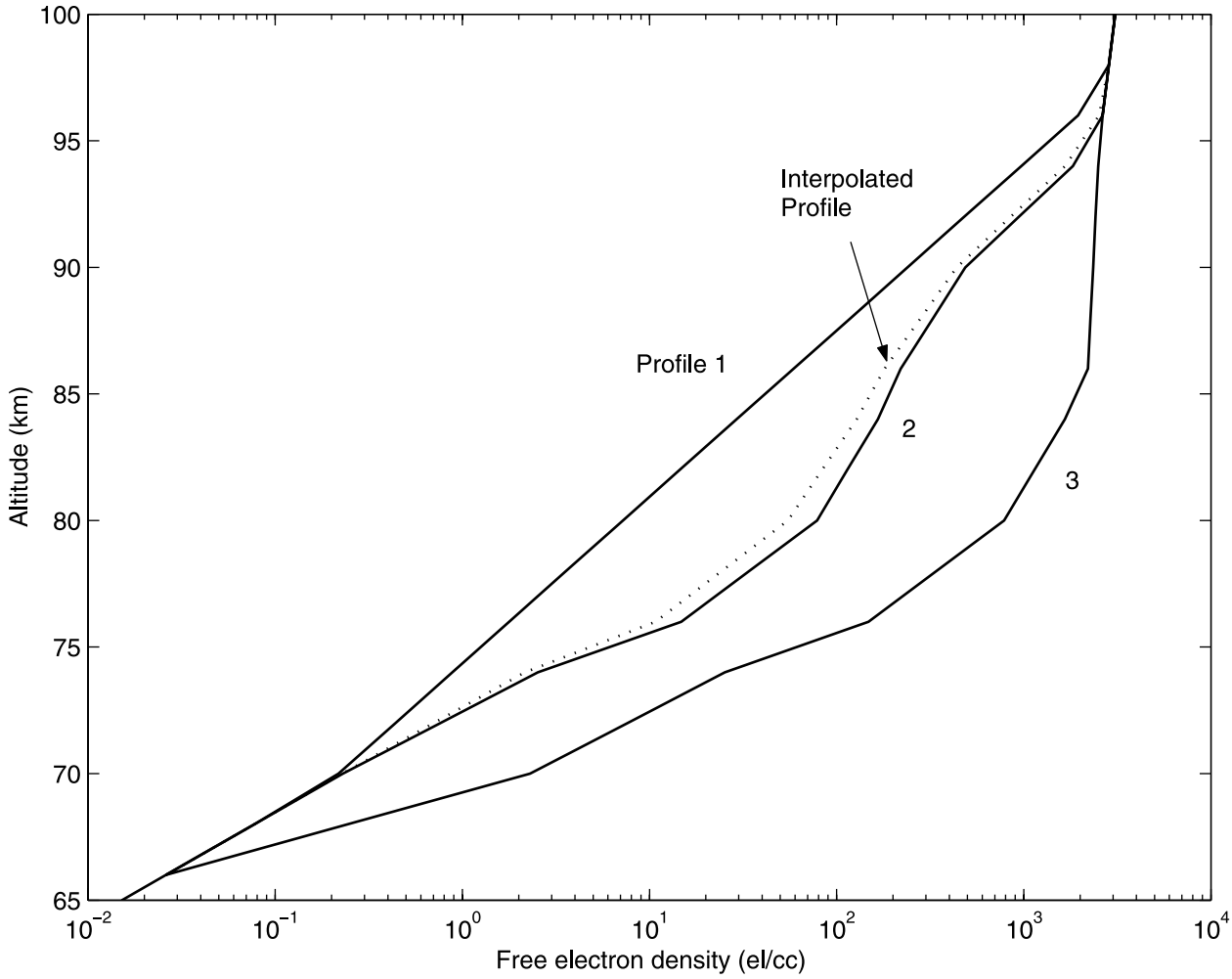

Figure 12. The three different nighttime electron density profiles for the *D* region (as in Figure 5) used in this paper, and the interpolated profile which best fits the HAIL measurements at 08:15 UT, July 4, 2001.

velocities of 1.0017 and 1.0141 c, respectively. The spacing between peaks (or nulls) in the interference pattern is given by

$$\ell = 2\pi/\Delta k, \text{ where } \Delta k = 2\pi f \cdot (1/v_2 - 1/v_1)$$
$$= \frac{2\pi f}{v_1 v_2}(v_1 - v_2), \quad (9)$$

which equals 1018 km. Therefore measurements over a 1000 km segment of the propagation path would directly reveal the difference in phase velocity of QTM_1 and QTM_2. Further information can be extracted with additional calculations, as described below.

[33] Each waveguide mode is characterized by four parameters: amplitude, phase offset, phase velocity, and attenuation rate (with distance). At each site we measure two values: amplitude and phase of the sum of the modes. Therefore, to solve for M modes, we need measurements at $N \geq 2M$ sites. Let A_i be the complex signal amplitude (thus incorporating amplitude and

Table 5. Discrepancy Between Measured Phase 07:15–09:15 UT and Best Fit Profile for 08:15 UT

Time, UT	Mean Phase Difference	Mean Absolute Phase Difference
07:15	2.3	7.8
07:45	1.6	6.8
08:15	−1.0	4.7
08:45	−40.1	43.9
09:15	−38.3	38.4

phase) measured at the i'th receiver (where $i \leq N$). This measured value is the sum of M modes:

$$A_i = \sum_{m=1}^{M} A_m \exp(-jk_m z_i), \tag{10}$$

where A_m is the complex amplitude of the m'th mode, k_m is the complex wavenumber of the m'th mode (incorporating phase velocity and attenuation), and z_i is the great-circle path length from the transmitter to the i'th receiver.

[34] In matrix notation,

$$\overline{A_i} = \overline{\overline{K}}\,\overline{A_m}, \tag{11}$$

where $k_{im} \equiv \exp(-jk_m z_i)$. In order to find a meaningful solution we require N $\geq$ 2M, which means that $\overline{\overline{K}}$ is not a square matrix. If $\overline{\overline{K}}$ was a square matrix, we could write

$$\overline{A_m} = \overline{\overline{K^{-1}}}\,\overline{A_i} \tag{12}$$

and find a set of mode amplitudes which would fit the data exactly, for any k_m. If any arbitrary set of k_m values could be made to fit the data, we would not obtain any information about the real k_m. However, for N $\geq$ 2M, we have

$$\overline{A'_m} = \overline{\overline{K^{\dagger}}}\,\overline{A_i}, \tag{13}$$

where $\overline{\overline{K^{\dagger}}} \equiv \left(\overline{\overline{K^T}}\,\overline{\overline{K}}\right)^{-1}\overline{\overline{K^T}}$, the left pseudo-inverse of $\overline{\overline{K}}$. Using equation (13) gives the mode amplitudes which best fit the data, for a given set of k_m values. Our goal is to find the k_m which minimizes the error vector

$$\overline{E} = \overline{A_i} - \overline{\overline{K}}\,\overline{A'_m} \tag{14}$$

$$= \overline{A_i} - \overline{\overline{K}}\,\overline{\overline{K^{\dagger}}}\,\overline{A_i}. \tag{15}$$

Note that $\overline{\overline{K}}\,\overline{\overline{K^{\dagger}}}$ is not an identity matrix. While $\overline{\overline{K^{\dagger}}}\,\overline{\overline{K}}$ is an M-by-M identity matrix, $\overline{\overline{K}}\,\overline{\overline{K^{\dagger}}}$ is an arbitrary N-by-N symmetric matrix, for which we want $\overline{A_i}$ to be an eigenvector with an eigenvalue of 1.

[35] Ideally we can make $||\bar{E}|| = 0$ by choosing the right k_m, but in the presence of noise there will necessarily be some irreducible error $||\bar{E}|| = \eta$. Also, since we have a finite number of receivers, we can only solve for a finite number of modes, and any additional modes present in the signal will appear as noise, and contribute to η. This error value provides a criterion for assessing the quality of the mode solutions. Elements of $\overline{A'_m}$ with magnitude less than η may be considered spurious solutions.

8. Mode Solutions and Array Geometry in the Presence of Noise

[36] Recalling that we need $N \geq 2M$ receivers to solve for M modes, and that the HAIL array presently has 13, one might at first think that it would be possible to solve for up to 6 modes. However, we need to recognize that the presence of noise renders some of our measurements no longer independent. Referring to Figures 10 and 11, we can see that the model data vary smoothly with distance, while the measured data do not. This is because the measurements consist of the NAA signal plus noise, while the model data represent only an idealized signal. Signals at nearby stations are highly correlated, whereas noise measurements are independent. Based on a given mode constellation and noise level, we can define a correlation distance within which measurements are not independent, in the sense that the difference in signal is less than the measurement uncertainty. For the data shown in Figure 11, the mean absolute phase difference between the measured data and the best fit model is 4.7 degrees, and the mean absolute phase slope with distance is 0.17 degrees/km. Assuming the best fit model is a good representation of the NAA signal, this gives a correlation distance of 27 km. Boulder, Green Mountain, Colorado Springs, and Pueblo all lie within this distance of each other (in terms of path length to NAA), so their data values effectively constitute only a single measurement of the NAA signal. The same is true of Walsenburg and Trinidad. This leaves only five independent measurements in this data set.

[37] With five independent measurements one might be tempted to conclude that one can solve for two modes. However, when we attempt to do so, all other modes (which are not measured) appear as noise, and add to the measurement uncertainty. When we set out to solve for two modes, we implicitly assume that the measured values consist of a sum of only those two modes. Since such is not the case at the HAIL sites for the NAA signal, our result end up being inaccurate. We can further illustrate the inherent difficulty of solving for mode properties by considering what it would take to solve for just one mode. The measured phase values over the range of HAIL sites as shown in Figure 11 follow an approximately linear trend, so that in the absence of other information we might conclude (based on the measurements at HAIL sites alone) that the signal consists of only a single mode. Fitting a line to this data over the limited HAIL range yields a phase velocity of 1.0059 c. However, such a measurement is clearly not meaningful, since it is evident from Figure 7 that if we measured the slope in a different limited range we would get a quite

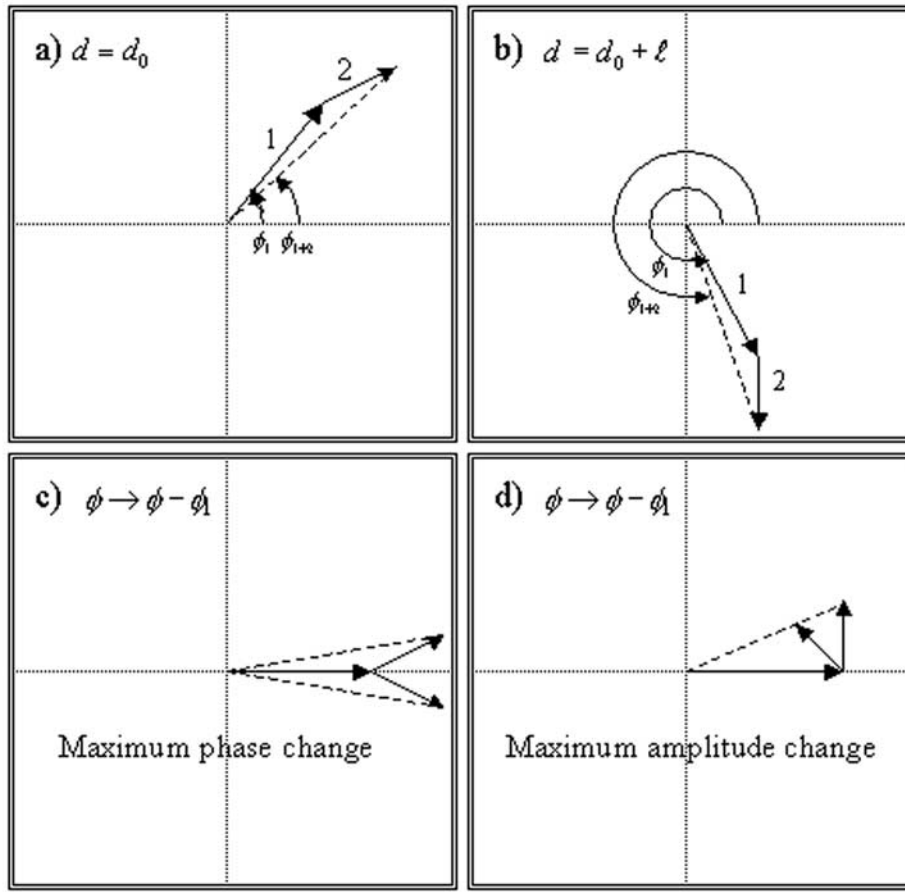

Figure 13. Examples of the phasor sum of modes. (a) Two hypothetical mode phasors measured at one end of the array (minimum distance to transmitter $d = d_0$). (b) The mode phasors at the other end (maximum distance $d = d_0 + \ell$). (c) The two sets of phasors superimposed, with the phase of the larger mode subtracted, to show the change in phase of the sum due to the presence of the smaller mode. In this case the two phasors are aligned, so that the total phase change is maximized and amplitude change is minimized. (d) The opposite case.

different value. The parameters of waveguide modes are in general not individually separable. What is required is adequate sampling of the mode interference pattern, so that we can simultaneously solve for all significant components of the signal.

[38] We now need to define what we mean by adequate sampling. According to the equations in the previous section, in the absence of noise or measurement error, given a finite number of modes M, and a sufficient number of receivers $N \geq 2M$, we can find the correct mode parameter values (for which $\|\bar{E}\| = 0$), regardless of where the receivers are located. However, if the variation in signal properties between sites is less than the measurement uncertainty, the number of independent measurements is reduced, in effect reducing N. Accurate determination of the mode properties requires that the $N \geq 2M$ criterion is maintained, even in the presence of noise.

[39] The presence of noise imposes other restrictions. First, the amplitude of each particular mode must be above the noise level, in order for it to be reliably detected. Furthermore, if the change in relative phase of two modes over the length of the array is less than the uncertainty of the phase measurements, then the phase velocities of those two modes are not separable, and they appear as one mode, whose amplitude and phase are the result of the phasor sum of the two modes. The change in total amplitude and phase over the length of the array depends on the amplitudes and original phase difference of the two modes, as shown in Figure 13.

Table 6. Best Fit Parameters for Two Modes at 08:15 UT

Mode	v_ϕ/c	α, dB/Mm	Relative Amplitude
1	1.0013	−5	1
2	1.0260	0	0.428

[40] Simple calculations, based on the phasor geometry and the assumption of uniform random distribution for the original phase difference of the two modes, show that the expectation value of phase change in the sum due to the presence of the smaller mode is

$$\overline{\Delta\phi} \approx \frac{2}{\pi}\frac{A_2}{A_1}\Delta k \cdot \ell, \text{ for } A_2 < A_1 \text{ and } \Delta k \cdot \ell < \pi/2 \quad (16)$$

$$= 4f\frac{A_2}{A_1}\frac{v_2 - v_1}{v_1 v_2} \cdot \ell, \quad (17)$$

or

$$\approx \frac{2}{\pi}\frac{A_2}{A_1}, \text{ for } A_2 < A_1 \text{ and } \Delta k \cdot \ell > \pi/2, \quad (18)$$

where A_1, A_2 are the mode amplitudes, v_1, v_2 are the mode phase velocities, and ℓ is the length (or range extent) of the measurement array in the direction of wave propagation, i.e., the difference in transmitter-receiver path length between the closest and farthest sites.

[41] For the HAIL array, we have (ℓ = 293 km. Based on equation (17) and the mode parameters in Table 2 (typical nighttime ionosphere), the expected phase difference of the two largest modes (QTM_1 and QTM_2) over an array of this length is 26 degrees. Such a phase difference should be detectable, given a phase uncertainty of 5 degrees. For QTM_1 and QTE_2 (the third-largest mode), $\overline{\Delta\phi}$ = 5.3 degrees, barely detectable. The phase velocity of the third and fourth largest modes, QTE_1 and QTE_2 are very close to one another. For these two, $\overline{\Delta\phi}$ = 1.3 degrees, so they are not separable from each other, and appear as a single mode. For QTM_1 and QTM_3 (the fifth-largest mode), $\overline{\Delta\phi}$ = 4.8 degrees, based on equation (18).

[42] The above considerations suggest that, with the present set of HAIL measurements in hand, we can resolve at least the two largest nighttime modes on the HAIL array, since their phase velocities are separable, and we have sufficient independent data points to satisfy $N \geq 2M$, for M = 2. Applying the method described in the previous section to the data at 08:15 UT (shown in Figures 10 and 11), we obtain the waveguide mode parameters listed in Table 6. For comparison we computed the waveguide mode parameters for the best fit ionospheric profile described by equation (8). The parameters of the two largest modes are listed in Table 7.

Table 7. LWPC Calculated Mode Parameters for Best Fit Profile at 08:15 UT

Mode	v_ϕ/c	α, dB/Mm	Relative Amplitude
QTM_1	1.0016	−2.6	1
QTM_2	1.0137	−4.9	0.370

[43] The two methods give almost the same value for the phase velocity of the largest mode (QTM_1). However, they give different values for the phase velocity and amplitude of the second mode. The values for Mode 2 in Table 6 are based on an unresolved sum of higher-order modes, including QTM_2 as well as higher modes. In this sense, we should not expect agreement between the values calculated for the specific QTM_2 mode as given in Table 7.

[44] The attenuation values in Table 6 are relatively inaccurate for two reasons. First, uncertainty in the amplitude measurements creates uncertainty in the attenuation values. An uncertainty of 10% in amplitude corresponds to 2.8 dB/Mm uncertainty in attenuation over the length of the HAIL array (293 km), a value which is comparable to the theoretical values of attenuation constants given in Table 7. Secondly, the interference pattern of unresolved modes (i.e., those other than QTM_1 and QTM_2) creates variations in amplitude along the length of the array, which cannot be distinguished from attenuation effects in our data set, which represents samples over a very limited segment of the great circle path.

[45] Table 8 shows the parameters for two modes measured after sunrise, at 08:45 UT. These values are shown for the sake of completeness, although it is difficult to interpret them on a physical basis, since (1) we do not have LWPC mode values to compare them to, (2) we cannot make the same argument that two modes should be resolvable as we did for the data at 08:15 UT, and (3) they represent at most two of the modes existing at this time, and not the complete mode structure. In order to extract useful information about the state of the lower ionosphere at this time, we would require a different array geometry, specifically configured for waveguide mode measurements. The design of such an array is described in the Summary and Conclusions section.

[46] Despite the cited limitations of the method and the lack of proper sampling of the mode interference pattern

Table 8. Best Fit Parameters for Two Modes at 08:45 UT

Mode	v_ϕ/c	α, dB/Mm	Relative Amplitude
1	0.9989	−8	1
2	1.0060	−5	0.718

with the present HAIL constellation of sites, the QTM_1 phase velocity and attenuation values measured at 08:15 UT (Table 6) were derived from raw data with only a few assumptions. To our knowledge, these values constitute the first direct measurement of the parameters of individual VLF waveguide modes propagating in the Earth-ionosphere waveguide. With the present array, it is possible to resolve only certain modes under certain ionospheric conditions (based on relative phase change, as in equations (16)–(18)), but with a longer array it would be possible to resolve several modes for an arbitrary ionosphere, as discussed below.

9. Other Transmitter Signals

[47] In this paper we analyze only the NAA signal in detail although the amplitude and phase of several other VLF transmitters are routinely recorded with the HAIL array. The analysis of other transmitter signals (see Introduction and Figure 1) presents additional challenges, as detailed below, and may be the subject of other studies.

[48] The 24.8 kHz NLK transmitter in Jim Creek, Washington: Other LWPC calculations (not shown) indicate that since the NLK transmitter is closer to the HAIL array than NAA, higher-order waveguides modes excited at the transmitter are less attenuated. As a result, more than 10 significant modes are present nighttime in the signal received at HAIL sites, so that we would need at least 20 receivers (spread over a distance of order 1000 km) to measure their parameters. However, the method of determination of a lower ionospheric profile by means of fitting amplitude/phase values to those calculated with LWPC (as in Figures 10–12) should in principle still be applicable.

[49] The 40.75 kHz NAU transmitter in Aquadilla, Puerto Rico: The NAU signal also contains over 10 significant modes, despite the long path length, because of the higher operating frequency (40.75 kHz). Again the present HAIL sites do not allow enough resolution for the mode-fitting method to be applicable. The profile-fitting method is also questionable, because the relatively longer path length challenges the assumption of a homogeneous ionosphere along the entire path. The NAU signal may also be more sensitive to variations along the path because of its shorter wavelength.

[50] The 21.4 kHz NPM transmitter in Lualuauei, Hawaii: LWPC calculations indicate that the nighttime NPM signal received at HAIL should consist of only 4 significant modes. However, the generally north-south orientation of the HAIL array is not favorable to resolve the individual waveguide modes of the NPM signal, in that the array is nearly aligned with the NPM-HAIL wavefront. The maximum difference in path length among the HAIL sites is only 87 km for NPM, versus 293 km for NAA. Relative phase variations of modes along the array are proportionally smaller, and by equation (17) are therefore difficult to detect, hampering both the mode-fitting and profile-fitting methods. The long path length (from Hawaii to Colorado) presents additional difficulties in fitting a single profile in the context of a homogeneous ionosphere assumption.

10. Summary and Conclusions

[51] We have used phase-coherent VLF data recorded at multiple sites to determine the nighttime lower ionospheric electron density profile in effect at the time, showing that the relative VLF phase and amplitude measurements at different sites provides a highly sensitive method for assessment of the electron density profile in the nighttime *D* region. This method is based on comparing the amplitude/phase values calculated using VLF propagation models to those measured at multiple sites, and iterative- adjustment of the altitude profile used for model calculations until a good fit is obtained. The one case analyzed here indicated a correspondence in both amplitude (±10%) and phase (±5 degrees) between the HAIL data and the predictions of a model of VLF propagation in the Earth-ionosphere waveguide, using a laterally homogeneous ionosphere, with an electron density versus altitude profile based on models used in previous work. The geometry of the present HAIL array is quite adequate for this method, and in fact the result shown in this study could have been obtained with even fewer receivers. However, for this purpose, it would be better if the array extended in a line along the direction of wave propagation, so as to minimize errors due to lateral variations in the ionosphere.

[52] We have also described a new method for determination of the parameters (phase velocity and attenuation rate) of individual waveguide modes which constitute the VLF signal propagating in the Earth-ionosphere waveguide. Parameters for two individual waveguide modes were determined independently of any assumed ionospheric profile and without using any VLF propagation model. Based on the methodology put forth, measurements of the mode interference pattern require the use of an array expressly designed for the purpose. The HAIL array was laid out so as to optimize the determination of the lateral extent of transient and localized ionospheric disturbances, and the distance range covered in the direction of signal propagation does not allow sufficient sampling of the waveguide mode interference pattern.

[53] The decomposition of the signal into its individual component waveguide modes can potentially allow the extraction of more information than iterative determination of the profile based on total amplitude/phase measurements. However, identification of all of the significant modes would require a different configuration of measure-

ment sites, with the following characteristics: (1) receiver sites aligned in the direction of wave propagation (or best compromise in view of the desirability of measuring signals from multiple transmitters), (2) sufficient number of receivers to solve for all significant modes ($N \geq 2M$), (3) sufficient overall spatial extent and site spacing to sample the main features of the mode interference pattern, (4) sufficient extent and site spacing to resolve the minimum and maximum differences in mode phase velocity, and (5) spatial extent no greater than necessary, to minimize variations in the ionosphere over the array.

[54] To measure the NAA signal at distances of approximately that of the HAIL array, these criteria point to $\sim$20 measurement sites spaced $\sim$50 km apart and with a total spatial extent of $\sim$1000 km. The preliminary results of this study lay the groundwork for the determination of the ambient nighttime *D* region profiles in near-real time, so that these profiles can be made available as Space Weather data.

[55] Only the volume of data and processing time restricts the possible use of multiple-site VLF measurements for near-real time remote sensing of the nighttime *D* region. With present facilities it is practical to record 1 s of broadband data (200 kilobytes) every hour at each station, indefinitely, and to compute the mode structure at selected times from the archived data. The next technological advance would be to automatically compute the mode structure and ionospheric profile, without having to record the wideband data. Knowing the ambient profile and mode structure would make possible an entirely new generation of quantitative analysis of transient disturbances such as lightning-induced electron precipitation events. Furthermore, the 1 s per hour data may be augmented with continuous broadband recordings on selected nights, in order to make interferometeric measurements of localized ionospheric disturbances produced in association with lightning discharges.

[56] **Acknowledgments.** This research was supported by the National Science Foundation under grant ATM-9910532 and by the Office of Naval Research under grant N00014-94-1-0100. We thank Mike Johnson and Robert Moore for their contributions to the development of the HAIL array, and Michael Chevalier and Robert Moore for running the LWPC calculations used in this paper. We further thank Robert Moore for his outstanding work in developing the HAIL data acquisition software.

References

Baba, K., D. Nunn, and M. Hayakawa, The modeling of VLF Trimpis using both finite element and 3-D Born modeling, *Geophys. Res. Lett.*, *25*, 4453, 1998.

Barr, R., M. T. Reitveld, P. Stubbe, and H. Kopka, The diffraction of VLF radio waves by a patch of ionosphere illuminated by a powerful HF transmitter, *J. Geophys. Res.*, *90*, 2861, 1985.

Bell, T. F., R. A. Helliwell, U. S. Inan, and D. S. Lauben, The heating of suprathermal ions above thunderstorm cells, *Geophys. Res. Lett.*, *20*, 1991, 1993.

Bell, T. F., U. S. Inan, M. T. Danielson, and S. A. Cummer, VLF signatures of ionospheric heating by HIPAS, *Radio Sci.*, *30*, 1855, 1995.

Budden, K. G., The influence of the Earth's magnetic field on radio propagation by waveguide modes, *Proc. R. Soc. London, Ser. A*, *265*(1323), 538, 1962.

Burgess, W. C., and U. S. Inan, The role of ducted whistlers in the precipitation loss and equilibrium flux of radiation belt electrons, *J. Geophys. Res.*, *98*, 15,643, 1993.

Cummer, S. A., Modeling electromagnetic propagation in the Earth-ionosphere waveguide, *IEEE Trans. Antennas Propag.*, *48*(9), 1420, 2000.

Cummer, S. A., T. F. Bell, and U. S. Inan, Mapping of the auroral electrojet using VLF measurements, in *Proceedings of the Second International Conference on Substorms*, p. 519, Univ. of Alaska Press, Fairbanks, 1994.

Cummer, S. A., T. F. Bell, and U. S. Inan, VLF remote sensing of high-energy auroral particle precipitation, *J. Geophys. Res.*, *102*, 7477, 1997.

Demirkol, M. K., U. S. Inan, T. F. Bell, S. G. Kanekal, and D. C. Wilkinson, Ionospheric effects of relativistic electron enhancement events, *Geophys. Res. Lett.*, *26*, 3557, 1999.

Ferguson, J. A., Computer programs for assessment of long wavelength radio communications, Version 1.0: User's guide and source files, *TD 3030*, Space and Nav. Warfare Syst. Cent., San Diego, Calif., 1998.

Ferguson, J. A., and F. P. Snyder, Computer programs for assessment of long wavelength radio communications, Version 1.0: Full FORTRAN code user's guide, *TD 1773*, Nav. Ocean Syst. Cent., San Diego, Calif., 1990.

Inan, U. S., D. L. Carpenter, R. A. Helliwell, and J. P. Katsufrakis, Subionospheric VLF/LF phase perturbations produced by lightning-whistler induced particle precipitation, *J. Geophys. Res.*, *90*, 7457, 1985.

Inan, U. S., J. V. Rodriguez, S. Lev-Tov, and J. Oh, Ionospheric modification with a VLF transmitter, *Geophys. Res. Lett.*, *19*, 2071, 1992.

Kikuchi, T., and D. S. Evans, Quantitative study of substorm-associated VLF phase anomalies and precipitating energetic electrons on November 13, 1979, *J. Geophys. Res.*, *88*, 871, 1983.

Lev-Tov, S. J., U. S. Inan, A. J. Smith, and M. A. Clilverd, Characteristics of localized ionospheric disturbances inferred from VLF measurements at two closely spaced receivers, *J. Geophys. Res.*, *101*, 15,737, 1996.

Nunn, D., K. Baba, and M. Hayakawa, VLF Trimpi modelling on the path NWC-Dunedin using both finite element and 3D Born modelling, *J. Atmos. Sol. Terr. Phys.*, *60*, 1497, 1998.

Pappert, R. A., and J. A. Ferguson, VLF/LF mode conversion model calculations for air-to-air transmissions in the Earth-ionosphere waveguide, *Radio Sci.*, *21*, 551, 1986.

Pappert, R. A., and D. G. Morfitt, Theoretical and experimental sunrise mode conversion results at VLF, *Radio Sci.*, *10*, 537, 1975.

Pappert, R. A., and F. P. Snyder, Some results of a mode-conversion program for VLF, *Radio Sci.*, *7*, 913, 1972.

Poulsen, W. L., T. F. Bell, and U. S. Inan, Three-dimensional modeling of subionospheric VLF propagation in the presence of localized *D* region perturbations associated with lightning, *J. Geophys. Res.*, *95*, 2355, 1990.

Poulsen, W. L., U. S. Inan, and T. F. Bell, A multiple-mode three dimensional model of VLF propagation in the Earth-ionosphere waveguide in the presence of localized *D* region disturbances, *J. Geophys. Res.*, *98*, 1705, 1993a.

Poulsen, W. L., T. F. Bell, and U. S. Inan, The scattering of VLF waves by localized ionospheric disturbances produced by lightning-induced electron precipitation, *J. Geophys. Res.*, *98*, 15,553, 1993b.

Reagan, J. B., R. E. Meyerott, R. C. Gunton, W. L. Imhof, E. E. Gaines, and T. R. Larsen, Modeling of the ambient and disturbed ionospheric media pertinent to ELF/VLF propagation, paper presented at Meeting on Medium, Long, and Very Long Wave Propagation, Adv. Group for Aerosp. Res. and Dev., N. Atl. Treaty Org., Brussels, Belgium, Sept. 1981.

Rodriguez, J. V., and U. S. Inan, Electron density changes in the nighttime *D* region due to heating by very low frequency transmitters, *Geophys. Res. Lett.*, *21*, 93, 1994.

Sechrist, C. F., Jr., Comparison of techniques for measurement of the *D* region electron densities, *Radio Sci.*, *9*, 137, 1974.

Smith, A. J., and P. D. Cotton, The Trimpi effect in Antarctica: Observations and models, *J. Atmos. Terr. Phys.*, *52*, 341, 1990.

Wait, J. R., A possible mechanism for excessive mode conversion in the Earth-ionosphere waveguide, *Radio Sci.*, *1*, 1073, 1966.

Wait, J. R., and K. P. Spies, Influence of finite ground conductivity on the propagation of VLF radio waves, *Tech. Note 300*, Natl. Bur. of Stand., Washington, D. C., 1964.

G. Bainbridge, SRI International, 333 Ravenswood Ave., Menlo Park, CA 94025, USA. (geoff_bainbridge@yahoo.com)

U. S. Inan, Space, Telecommunications, and Radioscience (STAR) Laboratory, Stanford University, Stanford, CA 94305, USA.